

# Performance Analysis of PLAXIS Models of Stone Columns in Soft Marine Clay



M. Vinoth, P. S. Prasad and U. K. Guru Vittal

**Abstract** The behavior of stone columns in soft marine clay under a cement concrete road pavement was examined through PLAXIS 2D. It is a well-known fact that modeling in 2D will require less computational effort compared to a full 3D analysis. The main difficulty with regard to PLAXIS 2D modeling of stone columns is the conversion of the stone column grid to a 2D stone trench structure. Different approaches (enhanced soil parameter, embedded beam element and equivalent column method) are available in modeling of stone column in PLAXIS 2D. However, not much literature is available for choosing the proper approach in PLAXIS 2D modeling of stone column in soft marine clay. The aim of this paper is to establish the suitable approach which provides better results with minimal effort for modeling in PLAXIS 2D. A case study, of work carried out at Mumbai for the road pavement between Wadala Depot and Chembur, provides the basis for PLAXIS 2D modeling. The sub-soil profile in this stretch comprises of soft marine clay, and the ground below cement concrete pavement had been treated with stone column prior to construction of rigid pavement. The results of the PLAXIS 2D models were then validated by examining the main characteristics of cement concrete pavement deformation within the column grid.

**Keywords** PLAXIS 2D · Stone column · Soft marine clay

---

M. Vinoth (✉) · P. S. Prasad · U. K. Guru Vittal  
CSIR—Central Road Research Institute, CRR I (PO), New Delhi 110025, India  
e-mail: [vinothm.27@gmail.com](mailto:vinothm.27@gmail.com)

P. S. Prasad  
e-mail: [pulikanti@gmail.com](mailto:pulikanti@gmail.com)

U. K. Guru Vittal  
e-mail: [vittal.crrl@gmail.com](mailto:vittal.crrl@gmail.com)

## 1 Introduction

Installation of stone columns in soft marine clay is very common as it increases the load carrying capacity of the foundation soil as well as provides the free drainage path for water to travel to the ground surface and reduces the post-construction settlements. In order to assess stone column performance through numerical modeling, designer has to go through one of the complex tasks, which is the conversion of the stone column grid to a two-dimensional (2D) stone trench structure. Earlier researchers have proposed several methods to convert the axisymmetric unit cell to the equivalent plane-strain model for the purpose of 2D numerical modeling of multi-drain field applications Hird et al. 1992; Indraratna and Redana 1997. These conversion methods involved the derivations of the equivalent plane-strain permeability or the equivalent plane-strain geometry based on the matching of axisymmetric and plane-strain consolidation analytical solutions. Numerical modeling by using finite-element software PLAXIS 2D 2015 provides three different approaches (enhanced soil parameter (ESP), embedded beam element (EBE) and equivalent column method (ECM)) for modeling stone column. Each one of these approaches has been separately used by various researchers Tan et al. (2008); Ng and Tan (2015) for modeling stone column, but a comparative study to bring out the best-suited method for this type of problems is not addressed. So, in the present study, performance of the three different approaches, were assessed using the field data obtained from the case history carried out at Mumbai for the road pavement between Wadala Depot and Chembur. The finite column permeability and smear effects are excluded from this study.

## 2 Case History Details

The soil profile considered for the present study is from the case history of Mumbai monorail project, Mumbai Prasad et al. (2016). The width of the six-lane concrete road is 11 m. The surcharge loading considered for the analysis is 44 kN/m<sup>2</sup> (including the dead load of pavements). Typical soil profile in this stretch is given in Table 1.

**Table 1** Typical soil profile

Type of soil	Layer Thickness	SPT 'N' value
Fill Soil	0.5–4.5	5–8
Soft Clay	0.5–12	3–6
Stiff Clay	7.5–16.5	5–45
CWR	13.5–16.5	>50
MWR	>10	>100

CWR—Completely weathered rock

MWR—Moderately weathered rock

The ground water level in the boreholes varied from 1.1 to 1.7 m from natural ground level (NGL). The stone columns are arranged in a triangular pattern. The diameter and spacing of stone columns are 0.9–2.5 m *c/c*, respectively. Depth of stone column from ground surface varies from 9 to 12 m. Six borehole data (BH-01, BH-02, BH-03, BH-04, BH-05, and BH-06) were considered for the comparative study.

### 3 Formulation of Equivalent Stiffness and Permeability

For ECM and EBE, the equivalent stiffness was arrived based on the approach proposed by Tan and Oo (2005). Priebe (1995) approach was used in arriving at the equivalent stiffness for ESP method. Permeability for all the three cases was arrived based on the approach suggested by Tan and Oo (2005). These approaches are reviewed here.

As per Tan and Oo (2005) approach, equal flow path length normal to the column perimeter can be obtained by considering the column width of plane-strain case equal to the axisymmetric column diameter, i.e.,

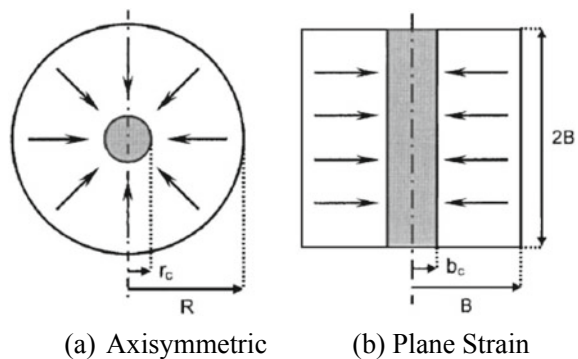
$$b_c = r_c \tag{1}$$

as shown in Fig. 1a,b. Similarly, Indraratna and Redana (2000) used this type of geometrical transformation in their permeability-matching approach for the plane-strain conversion of vertical drains. So, the equivalent plane-strain width *B* can be taken equal to the radius of drainage zone *R* [Fig. 1a,b], i.e.,

$$R = B \tag{2}$$

In general, this geometry conversion method is a very easy one since the transition between plane-strain meshed geometry and axisymmetric can be derived from the same basic (2D) input geometry.

**Fig. 1** Cross sections of unit-cell stone column and plane-strain conversions



Accordingly, material properties of plane-strain also need to be adjusted to account for the geometrical changes. By matching the column-soil composite stiffness, the following relationship can be used to arrive at the plane-strain material stiffness

$$E_{\text{composite}} = E_{c,ax}a_{s,ax} + E_{s,ax}(1 - a_{s,ax}) \quad (3)$$

where  $E_{\text{composite}}$  and  $E_s$  = elastic moduli of the composite material and the surrounding soil, respectively, and subscript ax denote axisymmetric conditions. Area replacement ratio  $a_s = A_c/(A_c + A_s)$ , where  $A_c$  and  $A_s$  = cross-section areas of the column and the surrounding soil, respectively. The composite stiffness obtained from Eq. (3) gives the average stiffness of the axisymmetric unit cell. The relevant stiffness of the stone column and the surrounding soil of the plane-strain model are computed by using the composite stiffness of the axisymmetric unit cell ( $E_{\text{composite}}$ ) obtained from Eq. (3). The relation for computation of stiffness of materials in the plane-strain unit cell is given by:

$$E_{\text{composite}} = E_{c,pl}a_{s,pl} + E_{s,pl}(1 - a_{s,pl}) \quad (4)$$

For simplicity,  $E_{s,pl} = E_{s,ax}$ , has been considered in this study. Hence  $E_{c,pl}$  can be determined from Eq. (4). The soil permeability was matched by using the following equation as derived by Tan and Oo (2005):

$$\frac{k_{h,pl}}{k_{h,ax}} = \frac{F(N)_{pl}}{F(N)_{ax}} \left[ \frac{m_{vs}m_{vc}(1 - a_s)}{m_{vc}(1 - a_s) + m_{vs}a_s} \right]_{pl} \left[ \frac{m_{vc}(1 - a_s) + m_{vs}a_s}{m_{vs}m_{vc}(1 - a_s)} \right]_{ax} \frac{B^2}{R^2} \quad (5)$$

where  $k_h$  = coefficient of soil permeability in horizontal direction;  $\alpha_{vc}$  and  $\alpha_{vs}$  = coefficients of compressibility of the column and the surrounding soil, respectively.  $F(N) = \left[ \frac{N^2}{(N^2-1)} \right] \ln(N) - \frac{(3N^2-1)}{4N^2}$ ; diameter ratio  $N = R/r_c$  for axisymmetric condition, whereas  $N = B/b_c$  for plane-strain condition;  $m_{vs} = \alpha_{vs}/(1 + e_s)$ ;  $m_{vc} = \alpha_{vc}/(1 + e_c)$ ; and  $e_c$  and  $e_s$  = void ratios of the columns and the surrounding soil, respectively. As, the influence of soil permeability in vertical direction  $k_{v,pl}$  is negligible when compared to horizontal, it is assumed that plane-strain vertical flow to be same as axisymmetric condition,  $k_{v,pl} = k_{v,ax}$ .

Priebe (1995) proposed improvement factors for soil improved through installation of stone columns. Improvement factors are evaluated on the assumption that the column material shears from the beginning while the surrounding soil reacts elastically. Furthermore, the soil is assumed to be displaced already during the column installation to such an extent that its initial resistance corresponds to the liquid state: i.e., the coefficient of earth pressure amounts to  $K = 1$ . The result of the evaluation is expressed as basic improvement factor  $n_0$ .

$$n_0 = 1 + \frac{A_c}{A} \cdot \left[ \frac{1/2 + f(\mu_s, A_c/A)}{K_{ac} \cdot f(\mu_s, A_c/A)} - 1 \right] \tag{6}$$

where  $f(\mu_s, A_c/A) = \frac{1-\mu_s^2}{1-\mu_s-2\mu_s^2} \cdot \frac{(1-2\mu_s) \cdot (1-A_c/A)}{1-2\mu_s+A_c/A}$ ;  $\mu$  = Poisson's ratio;  $K_{ac} = \tan^2(45^\circ - (\varphi_c/2))$ ;  $A$  = area of unit cell,  $A_c$  = cross-sectional area of single stone column. The columns materials are still compressible. This compressibility of the stone column material can be addressed by using a reduced improvement factor  $n_0$ . This can be arrived from the formula developed for the basic improvement factor  $n$ , when the given reciprocal area ratio  $A/A_c$  is increased by an additional amount of  $\Delta(A/A_c)$ .

$$n_1 = 1 + \frac{\bar{A}_c}{A} \cdot \left[ \frac{1/2 + f(\mu_s, \bar{A}_c/A)}{K_{ac} \cdot f(\mu_s, \bar{A}_c/A)} - 1 \right] \tag{7}$$

where  $\frac{\bar{A}_c}{A} = \frac{1}{A/A_c + \Delta(A/A_c)}$ ;  $\Delta(A/A_c) = \frac{1}{(A_c/A)_1} - 1$ ;

$$\left(\frac{A_c}{A}\right)_1 = -\frac{4 \cdot K_{ac} \cdot (n_0 - 2) + 5}{2 \cdot (4 \cdot K_{ac} - 1)} \pm \frac{1}{2} \cdot \sqrt{\left[\frac{4 \cdot K_{ac} \cdot (n_0 - 2) + 5}{4 \cdot K_{ac} - 1}\right]^2 + \frac{16 \cdot K_{ac} \cdot (n_0 - 1)}{4 \cdot K_{ac} - 1}}$$

The stone columns are better supported laterally with increasing overburden and, therefore, can provide more bearing capacity. Therefore, in order to consider this effect, depth factor  $f_d$  is calculated based on following equation and suitably applied to the improvement factor,

$$f_d = \frac{1}{1 + \frac{K_{oc} - W_s/W_c}{K_{oc}} \cdot \frac{W_c}{p_c}} \tag{8}$$

where  $p_c = \frac{p}{\frac{A_c}{A} + \frac{1-A_c/A}{p_c/p_s}}$ ;  $\frac{p_c}{p_s} = \frac{1/2 + f(\mu_s, \bar{A}_c/A)}{K_{ac} \cdot f(\mu_s, \bar{A}_c/A)}$ ;  $W_c = \sum(\gamma_c \cdot \Delta d)$ ;  $W_s = \sum(\gamma_s \cdot \Delta d)$ ;

$K_{oc} = 1 - \sin \varphi_c$ ;  $p$  = surcharge pressure,  $d$  = thickness of soil layer,  $\gamma_s$  and  $\gamma_c$  denote bulk densities of soil and column. In order to counter simplifications and approximations, compatibility controls have to be performed. This is to guarantee that the settlement of the stone columns resulting from their inherent compressibility does not exceed the settlement of the surrounding soil resulting from its compressibility by the loads which are assigned to each. So using the following equation, upper limit of improvement factor can be obtained,

$$n_{Gr} = 1 + \frac{A_c}{A} \cdot \left(\frac{D_c}{D_s} - 1\right) \tag{9}$$

where  $D_c$  and  $D_s$  are Young's moduli of stone column and soil, respectively. Final improvement factor is given by

$$n_2 = f_d \times n_1 \quad (10)$$

Therefore, enhanced stiffness of soil will be equal to existing soil stiffness multiplied by improvement factor  $n_2$ . Similarly, shear resistance from friction of the composite system can be calculated using the below equations:

$$\tan \bar{\varphi} = m' \cdot \tan \varphi_c + (1 - m') \cdot \tan \varphi_s \quad (11)$$

$$c' = (1 - m') \cdot c_s \quad (12)$$

where  $m' = (n - 1)/n$ ;  $n$  = improvement factor,  $\varphi_c$  and  $\varphi_s$  are the angles of internal friction of column and soil, respectively,  $c'$  = Cohesion of unimproved soil.

## 4 Settlement Calculation

Theoretical settlement was calculated by using Terzaghi's (1925) one-dimensional consolidation equation.

$$S_c = \sum_{i=1}^n \frac{C_{ci} H_{oi}}{1 + e_{oi}} \log \left( \frac{\sigma_{v'fi}}{\sigma_{v'oi}} \right) \quad (13)$$

where  $C_{ci}$  = compression Index of respective layer,  $H_{oi}$  = thickness of respective layer,  $e_{oi}$  = initial void ratio of respective layer,  $\sigma_{v'fi}$  = final vertical effective stress of respective layer,  $\sigma_{v'oi}$  = initial vertical effective stress of respective layer.

As per the reduced stress method, settlement reduction factor due to stone column installation was determined using the following equation,

$$\mu_g = \frac{n}{1 + (n - 1)a_s} \quad (14)$$

where  $n = \sigma_s/\sigma_g$ ;  $\sigma_s$  and  $\sigma_g$  are vertical stress in compacted columns and surrounding ground.

## 5 Numerical Modeling

Three different finite-element models of the stone column-improved soil section were considered: enhanced soil property, equivalent beam method and equivalent column method. The plane-strain modeling was chosen as the road spanned a

distance of about 8.5 km with almost uniform cross-sectional geometry in the direction normal to the plane. The plane-strain models were developed using 15-node triangular elements in PLAXIS 2D version 2015. For EBM and ECM, the width of stone columns was considered as 0.9 m, same that of axisymmetric condition. A spacing of 2.5 m was uniformly considered in all the embankment models. Self-soil weight was taken into account by applying the gravity effect, assuming the default gravity acceleration,  $g$ , is  $9.810 \text{ m/s}^2$ , and the direction is with the negative  $y$ -axis. Default unit weight of the water is  $10 \text{ kg/m}^3$ . In order to minimize the boundary effects, the overall geometry of the model was kept more than 5 times and 2.5 times the width of road in  $X$ -direction and  $Y$ -direction, respectively. During mesh generation stage, fine refinement was used so that more number of elements will be generated for obtaining more precise results. In order to simulate the dead load (self-weight of pavement layers) and live load at top a line load with an intensity of 44 kPa was applied. Parameters used for the analysis of BH-01 borehole data are listed in Table 2, where  $\gamma$  = bulk density;  $\phi'$  = angle of internal friction;  $c'$  = cohesion;  $E$  = Young's modulus or stiffness;  $\mu$  = Poisson's ratio;  $k_h$  and  $k_v$  are coefficients of permeability in vertical and horizontal directions, respectively.

The soft soils were modeled as undrained material in PLAXIS. Stone column for ECM was idealized as a homogeneous drained material having certain characteristics of stiffness and strength parameters. The elastic modulus of column material was taken as ten times that of soil. The compression index  $c_c$ , swell index  $c_s$ , and initial void ratio  $e_0$  of soft clay are 0.59, 0.144 and 1.973, respectively. The compression index  $c_c$ , swell index  $c_s$ , and initial void ratio  $e_0$  of stiff clay is 0.38, 0.125 and 1.438, respectively. Permeability in horizontal direction for soft clay is taken as twice of vertical direction. In order to avoid numerical complications, a small nonzero value has been considered for the strength parameters.

Plane-strain model parameters considered for both ECM and EBM are same, and the stiffness for both the method was determined using Eqs. (3) and (4). Permeability for all the three methods for modeling in PLAXIS 2D 2015 has arrived from Eq. (5). Shear parameters and stiffness values for embedded beam were selected as layer-dependent. Stiffness parameters for ESP method Eqs. (6)–(10) were used and shear parameter is used using Eqs. (11) and (12).

## 5.1 Simulation Procedures

The project involved the installation of stone columns and construction of six-lane concrete road over it was simulated as follows. The stone columns were first installed by partial soil replacement for ESP and ECM but for EBM embedded beam row is activated. Next-stage surcharge load (including the dead load of pavements) is activated. Last-stage consolidation process is carried out till the excess pore water pressure reduces to 1 kPa, and once this value is reached the analysis stops.

**Table 2** Material properties of all models—BH-01

Material	Model	Drain Type	$\gamma$ (kN/m <sup>3</sup> )	$\gamma_{sat}$ (kN/m <sup>3</sup> )	$\Phi^*$ (°)	$C^*$ (kPa)	$E$ (kPa)	$\mu$	$k_c$ (m/day)	$k_h$ (m/day)
Fill Soil#	HSM	Drained	18	18.75	29	0.1	11,500	0.3	8.64	8.640
Soft Clay <sup>a</sup>	SSM	Undrained (A)	15.6	15.6	1	13.5	3100	0.4	0.069	0.165
Stiff Clay <sup>b</sup>	SSM	Undrained (A)	16.6	16.6	1	22.5	6000	0.4	0.102	0.177
MWR	HSM	Undrained (B)	19.5	20.5	33	3500	1.43E + 07	0.25	0.1	0.033
Stone Column	MC	Drained	19	20	42	0.1	12,200	0.33	1	1.000
Embedded Beam	–	–	19	Layer Dependent	12,200	Layer Dependent				

# Values are only for ECM and EBM; corresponding for ESP model,  $E = 21,487$  kPa

<sup>a</sup>Values are only for ECM and EBM; corresponding for ESP model,  $E = 6107$  kPa and 8106 for above water table and below water table, respectively

<sup>b</sup>Values are only for ECM and EBM; corresponding for ESP model,  $E = 15,134$  kPa

HSM Hardening Soil Model; SSM Soft Soil Model; MC Mohr Coulomb



## 6 Results and Discussions

Analysis for all the six boreholes was done using all the three methods (i.e., ESP, EMB and ECM). Typical maximum settlement obtained from the analysis carried out using BH-01 has been shown in Fig. 2a–c. Theoretical settlements were calculated using Eqs. (13 & 14). All the analysis results along with theoretical and field values [obtained through leveling by Mumbai Mono Rail Development Authority in October 2010 and February 2015. This level difference as reported varies from 250 to 550 mm at different chain ages, Prasad et al. (2016)] are tabulated in Table 3.

From Table 3, it can be seen that out of three methods embedded beam method has better results than other two methods. One of the other interesting things we can notice is that theoretical predictions also vary with field values in the range of 16–56%. This variation is also erratic because in some cases it has over-predicted and in others underestimated. In cases where theoretical predictions are on higher end may be because the top fill layers would have dissipated the surcharge, leading to lower load intensity transferred to the soft soil layers and resulting in lesser settlement. Reason for under prediction may be the fill thickness is less than those considered for settlement calculation.

Except one borehole in all the other cases, ESP has underestimated settlement in the range of 40–90%. In EBM except for last borehole location in all other location, it has predicted settlement with just 25% variation. In ECM, constantly in all locations it has underestimated the settlement in the range of 50–90%.

It can be noted that for BH-05 and BH-06, all the methods including theoretical approach have underestimated the settlement. So this shows that actual thickness of fill and soft soil varies at site than what is considered for the study.

In order to explain the huge variation of settlement prediction among the three methods, each model's material stress state at the end of the analysis was studied. Figures 3a–c and 4a–c shows the elastic points and plastic points, respectively, at the end of simulation. It can be seen that EBM has very little elastic points and some plastic yielding in the surrounding region of the column material. It is clearly indicated by numerous plastic stress points that are concentrated within and slightly beyond the column periphery. The yielding pattern of the other two methods is almost the same but with less scatter beyond the column periphery and more plastic points; this explains the differential responses of the other two methods. The plastic yielding in the EBM allows itself to simulate the settlements of actual field case, while the other model's elasticity gives a stiffer response leading to a lower final settlement. The sustained elastic behavior in the ECM and ESP may be due to its larger cross-sectional column area with higher elastic capacity in both shearing and bending.

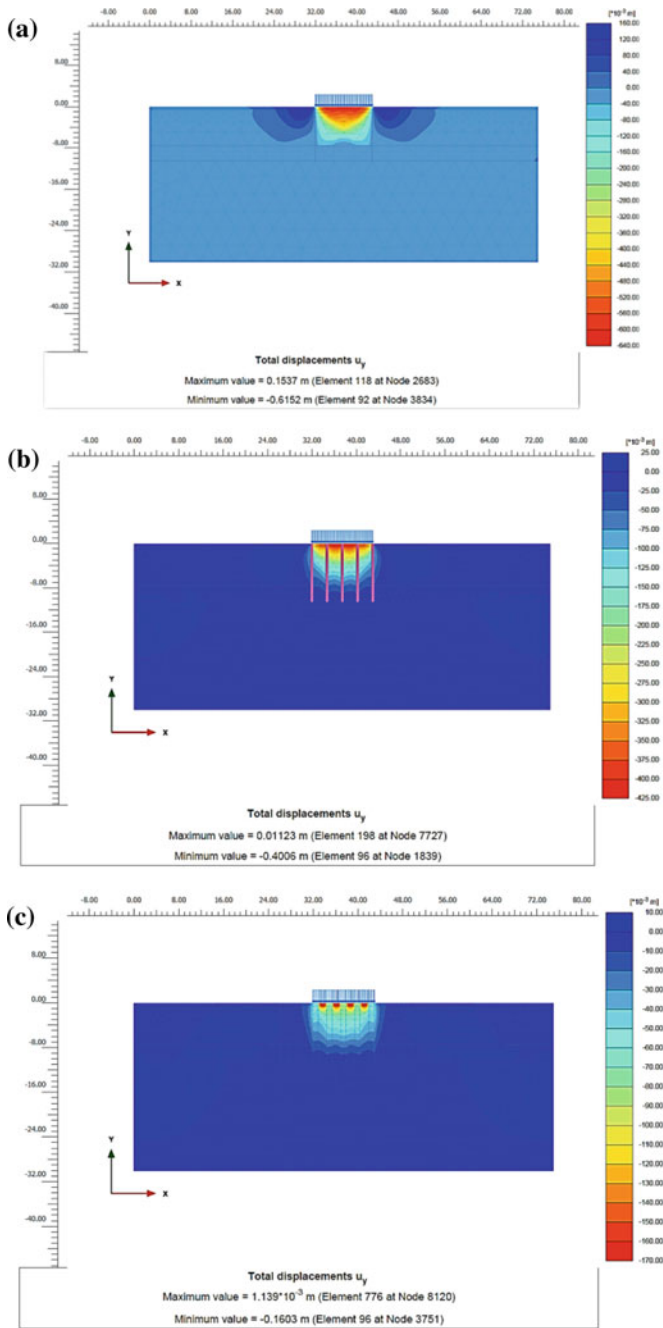
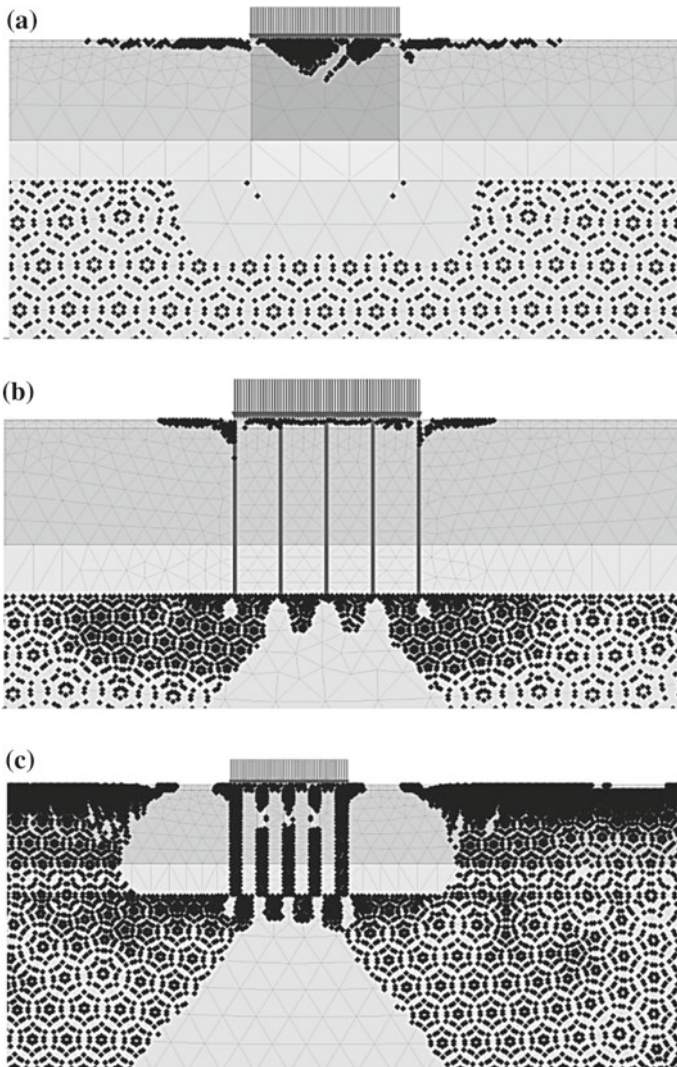


Fig. 2 a Displacement—ESP. b Displacement—EBM. c Displacement—ECM

**Table 3** Settlement comparison

Borehole	Theoretical	PLAXIS			Field <sup>a</sup>
		ESP	EBM	ECM	
BH-01	455.6	615.2	400.6	160.3	325
BH-02	349.0	147.1	209.3	100.8	300
BH-03	317.6	137.1	222.2	124.1	250
BH-04	390.9	181.2	226.1	76.52	300
BH-05	289.4	166.1	233.7	106.8	450
BH-06	258.1	39.55	103.6	41.22	450

<sup>a</sup>Prasad et al. (2016)



**Fig. 3** a Elastic Points—ESP. b Elastic points—EBM. c Elastic points—ECM

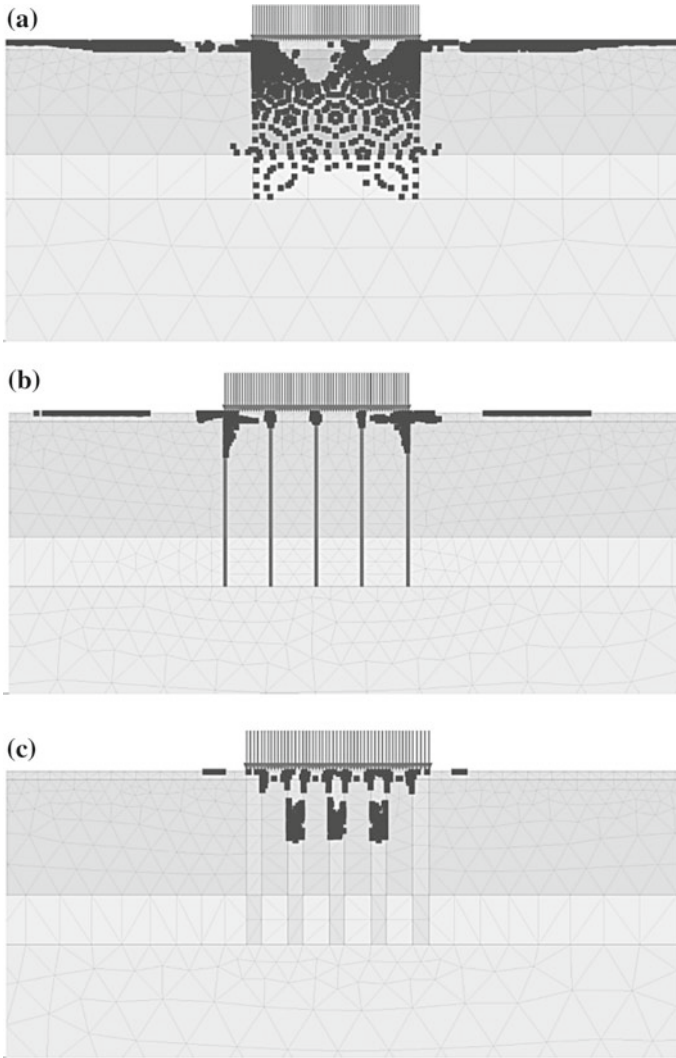


**Fig. 4** a Plastic points—ESP. b Plastic points—EBM. c Plastic points—ECM

## 7 Conclusion

This paper presents a comparative performance study of three different approaches (i.e., enhanced soil parameter, embedded beam element and equivalent column method) available in PLAXIS 2D 2015 version for assessing the settlement performance of stone column, by comparison with the field data, from a case history carried out at Mumbai for the road pavement between Wadala Depot and Chembur. Six borehole data were considered for the comparative study.

Stiffness and permeability of axisymmetric condition were converted into equivalent plane-strain values using Tan and Oo (2005) approach. Enhanced shear parameters of soil were also determined using Priebe (1995) approach. Theoretical settlement was calculated using Terzaghi's (1925) one-dimensional consolidation equation and settlement reduction factor due to stone column installation was determined using reduced stress method.

With all these data, analysis was carried out in PLAXIS 2D 2015. Following points can be brought out from the analysis results:

1. Out of three methods, embedded beam method has better results than other two methods. Except for the last borehole location in all other location, it has predicted settlement with just 25% variation.
2. Except one borehole in all the other cases, ESP has underestimated settlement in the range of 40–90%.
3. ECM constantly in all locations has underestimated the settlement in the range of 50–90%.
4. The plastic yielding in the EBM allows itself to simulate the settlements of actual field case, while the other model's elasticity gives a stiffer response leading to a lower final settlement. The sustained elastic behavior in the ECM and ESP may be due to its larger cross-sectional column area with higher elastic capacity in both shearing and bending.

Thus, embedded beam method is the preferred method for carrying out numerical modeling for elasto-plastic materials.

## References

- Hird CC, Pyrah IC, Russell D (1992) Finite element modelling of vertical drains beneath embankments on soft ground. *Geotechnique* 42(3):499–511
- Indraratna B, Redana IW (1997) Plane-strain modeling of smear effects associated with vertical drains. *J Geotech Geoenviron Eng* 123(5):474–478
- Indraratna B, Redana IW (2000) Numerical modeling of vertical drains with smear and well resistance installed in soft clay. *Can Geotech J* 37(1):132–145
- Prasad PS, Guru Vital UK, Sitaramanjaneyulu K, Madhav MR (2016) Remedial measures for upheaval of PQC panels adjacent to piers of Mumbai Monorail in Mumbai, 5th ICFGE-2016, Bangalore, India, pp 366–377
- Priebe HJ (1995) The Design of vibro replacement, *Ground Engineering*, Dec 1995, pp 31–37
- Tan SA, Oo KK (2005) Stone column FEM modeling—2D and 3D considerations illustrated by case history. In: *Proceedings of international symposium on tsunami reconstruction with geosynthetics*, ACSIG, Bangkok, Thailand, pp 157–169
- Tan SA, Tjahyono S, Oo KK (2008) Simplified plane-strain modeling of stone-column reinforced ground. *J Geotech Geo-Environ Eng*, ASCE 134(2):185–194
- Ng KS, Tan SA (2015) Simplified homogenization method in stone column designs. *Jpn Geotech Soc*, *Soils Found* 55(1):154–165
- Terzaghi K (1925) *Erdbaumechanik and bodenphysikalischer grundlage*, Deuticke, Lpz
- Terzaghi K, Peck RB, Mesri G (1996) *Soil mechanics in engineering practice*, Third Edition, Part II, *Theoretical soil mechanics*, John Wiley & Sons Inc, New York